P074

A Model-based Approach to the Common-diffraction-surface Stack

H. Shahsavani* (Shahrood University of Technology), J. Mann (Karlsruhe Institute of Technology), I. Piruz (Shahrood University of Technology) & P. Hubral (Karlsruhe Institute of Technology)

SUMMARY

The Common-Reflection-Surface stack method parameterizes and stacks seismic reflection events in a generalized stacking velocity analysis. It considers a discrete number of events contributing to a given stack sample such that conflicting dip situations can be handled. The reliable detection of such situations is difficult and missed contributions to the stacked section cause artifacts in a subsequent poststack migration. This is deleterious for complex data where prestack migration is no viable option due to its demands on velocity model accuracy, such that we might have to rely on poststack migration. As an alternative, the conflicting dip problem has been addressed by explicitly considering a virtually continuous range of dips with a simplified stacking operator in a process termed Common-Diffraction-Surface stack. In analogy to the Common-Reflection-Surface stack, the Common-Diffraction-Surface stack has been implemented and successfully applied in a data-driven manner based on coherence analysis in the prestack data. In view of the computational costs, we present a more efficient model-based approach to the Common-Diffraction-Surface stack designed to generate stack sections optimized to image discontinuities by poststack migration. This approach only requires a smooth macro-velocity model of minor accuracy. We present first results for a real land data set.

Introduction. The Common-Reflection-Surface (CRS) stack method follows the concept of the classical stacking velocity analysis, the local parameterization and stacking of reflection events by means of an analytic second-order approximation of the reflection traveltime (see, e. g., Mann et al., 1999). In its simplest implementation, the CRS stack determines only one optimum stacking operator for each zero-offset (ZO) sample to be simulated. Along this operator, we obtain the maximum coherence in the seismic reflection data. However, in the presence of curved reflectors or diffractors, various events might intersect each other and/or themselves, such that a single stacking operator per ZO sample is no longer appropriate. Thus, Mann (2001) proposed to allow for a small, discrete number of stacking operators for a particular ZO sample. The main difficulty in this approach is to identify conflicting dip situations and to decide how many contributions should be considered. This implies a tricky balancing between lacking contributions and potential artifacts due to the unwanted parameterization of spurious events. Soleimani et al. (2009) proposed an adapted CRS strategy designed to obtain a stacked section as completely as possible by merging concepts of the dip moveout correction with the CRS approach: instead of only a discrete number of dips and, thus, stacking operators per sample, a virtually continuous range of dips is considered. To simplify this process and to emphasize diffraction events, this has been implemented with a CRS operator reduced to (hypothetical) diffraction events: this Common-Diffraction-Surface (CDS) stack approach has been successfully applied to complex land data (Soleimani et al., 2010). However, the approach is quite time consuming, as separate stacking operators have to be determined for each stacked sample to be simulated and each considered dip in a data-driven manner by means of coherence analysis in the prestack data.

Here, we propose a model-based approach to the CDS stack. We assume that a smooth macro-velocity model has already been determined in which the parameters of the CDS stacking operators can be easily forward-modeled. This is far more efficient than the data-driven approach and further emphasizes diffraction events.

Traveltime approximation. The CRS method is based on an analytical approximation of the reflection traveltime up to second order in terms of the half source/receiver offset h and the displacement of the source/receiver midpoint x_m with respect to the location x_0 of the stacked trace to be simulated. For the 2D case considered in this paper, the hyperbolic CRS traveltime approximation can be expressed as

$$t^2(x_m,h) = \left[t_0 + \frac{2\sin\alpha}{v_0}(x_m - x_0)\right]^2 + \frac{2t_0\cos^2\alpha}{v_0}\left[\frac{(x_m - x_0)^2}{R_N} + \frac{h^2}{R_{NIP}}\right], \quad (1)$$

with v_0 denoting the near-surface velocity. The stacking parameter α is the emergence angle of the normal ray, whereas R_N and R_{NIP} are the local radii of hypothetical wavefronts excited by an exploding reflector experiment or an exploding point source at the (unknown) reflection point of the normal ray, the normal incidence point (NIP). All these properties are defined at the acquisition surface $(x_0, z = 0)$. For a true diffractor in the subsurface, an exploding point source experiment and an exploding reflector experiment naturally coincide such that $R_{NIP} \equiv R_N$. Thus, for *diffraction* events, the CRS traveltime equation (1) reduces to the CDS traveltime approximation

$$t^2(x_m,h) = \left[t_0 + \frac{2\sin\alpha}{v_0}(x_m - x_0)\right]^2 + \frac{2t_0\cos^2\alpha}{v_0 R_{CDS}}\left[(x_m - x_0)^2 + h^2\right], \quad (2)$$

with $R_{CDS} \equiv R_{NIP} \equiv R_N$. For *reflection* events, the CDS operator (2) is an inferior approximation compared to the full CRS operator (1) as $R_{NIP} \neq R_N$. Nevertheless, it still allows to approximate the event within a reasonably chosen aperture. For the data-driven CDS stack, this simplified operator has been chosen for performance reasons. For the model-based CDS stack, this simplification is mandatory, as there is no structural information on reflector curvatures contained in the considered smooth macro-velocity model. Thus, a forward-modeling of the lacking parameter R_N is not possible anyway. Note that in the data-based CDS stack, R_{CDS} represents a weighted average of R_N and R_{NIP}, whereas $R_{CDS} \equiv R_{NIP}$ in the model-based approach presented here. The difference between both definitions is significant!

Forward-modeling. The radius of the NIP wave occurring in the CDS operator (2) is associated with a hypothetical point source at the NIP. The local curvature of the corresponding wavefront is considered along the normal ray. Thus, the first step is to determine the potential normal ray by means of kinematic ray tracing. As we need this ray for a given surface location and a given emergence angle, the kinematic ray tracing is performed for the down-going ray. Kinematic ray tracing consists in the calculation of the characteristics of the Eikonal equation. We have chosen the particular system for which the variable along the ray is directly the traveltime, as we have to compute ray tracing results for a regular grid in ZO traveltime. The corresponding kinematic ray tracing system, in 2D a system of four coupled ordinary differential equations of first order, can be numerically integrated with the well known Runge-Kutta scheme of fourth order. The step length in the numerical solution is chosen as an integer fraction of the sampling rate of the stacked section to be simulated. In this way, we directly obtain discrete points along the ray paths corresponding to the desired output locations in the ZO time domain.

The determination of R_{NIP} requires dynamic ray tracing along the ray path. The 2D dynamic ray tracing system consists of two coupled ordinary differential equations of first order. For a given initial condition at a point of the ray, it allows to calculate the second partial derivative of traveltime normal to the ray for any point along the ray. For a point source initial condition at a NIP on the ray, this traveltime derivative is directly related to the searched-for stacking parameter. However, it is highly inefficient to integrate the dynamic ray tracing system upwards along the ray, as this had to be performed separately for each considered point on the ray, i. e., hundreds or thousands of times along each ray. Instead, it is far more efficient to perform the dynamic ray tracing in parallel to the kinematic ray tracing along the down-going ray twice, for two mutually orthogonal initial conditions: one corresponds to a point source, the other to a plane wave source at the emergence point of the ray. With the two orthogonal solutions along the ray, we can directly compute the solution for any arbitrary initial condition at any point of the ray, indeed also in its reverse direction. Thus, the searched-for solution for a point source at the NIP is readily available for all potential NIPs along the ray.

Implementation. The stacking parameter R_{NIP} varies smoothly for a smooth velocity model. Thus, ray tracing can be performed on a relatively coarse emergence angle grid. In contrast, the semblance and the stack itself are quite sensitive to variations of the emergence angle. Thus, stack and semblance are calculated on a finer emergence angle grid using linearly interpolated stacking parameters.

Although the stacking parameters do not have to be optimized as in the data-driven approaches, it is useful to calculate semblance along the individual CDS operators anyway. Note that this has to be performed only once per emergence angle for each ZO sample rather than dozens or hundreds of times as in the data-driven CDS stack, such that the semblance calculation is not a performance issue in the model-based case, but allows to keep track of the CDS operator yielding the highest semblance and its associated stacking parameters, emergence angle and NIP wave curvature, for the identification of ZO reflection events, the assessment of the quality of the operator fit, and plausibility analyses. The semblance associated with a particular CDS operator can be additionally used as a weight factor for its contribution to the final stack section, probably in combination with a semblance threshold.

First results. For the first application of the model-based CDS stack, we revisited the 2D land data set presented by Soleimani et al. (2009) in the context of the data-driven CDS stack, a line acquired by an energy resource company in fixed-spread geometry. For details on acquisition parameters and preprocessing, we refer to Soleimani et al. (2009). A sequence of CRS stack and NIP-wave inversion has been applied to the data to obtain the smooth macro-velocity model shown in Figure 1, see, e. g., Mann et al. (2003) for details on this workflow. Ray tracing is performed in this model for emergence angles $\pm 22°$ @ $2°$ spacing. The ray fan for one of the ZO trace locations is superimposed on the model in Figure 1. For the stack and the semblance calculation, we used emergence angles $\pm 20°$ @ $1°$ spacing.

Figure 2a shows the final result of the CRS stack. The reflection events show up with a high signal-to-noise ratio and high continuity. However, many events are truncated and only appear in fragments where they intersect more dominant events. This leads to artifacts in a subsequent poststack migration,

Macro-velocity model with superimposed ray fan
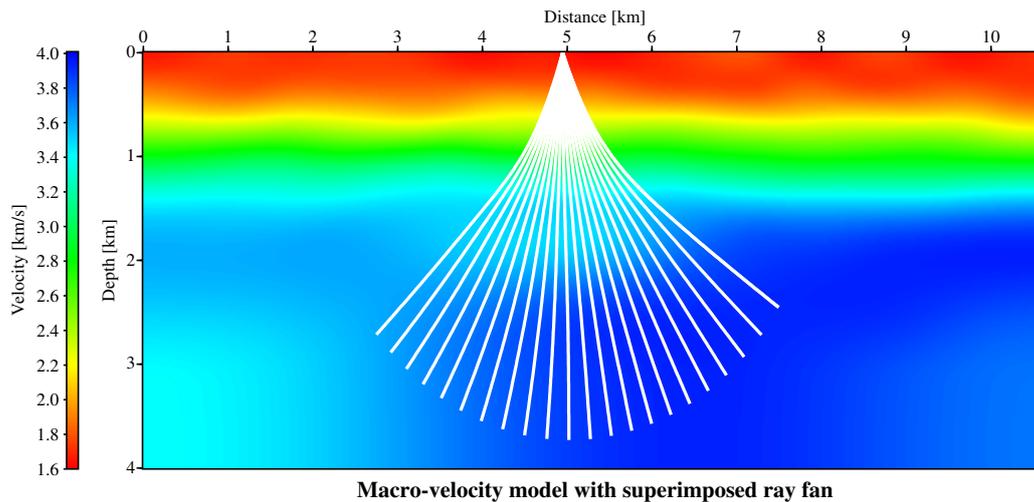
Figure 1: Macro-velocity model obtained by sequential application of CRS stack and NIP-wave inversion. For one emergence location, the ray fan for the coarse emergence angle grid is superimposed in white.

especially faults will be poorly imaged, as the corresponding edge diffractions are largely missing in the stacked section. In the data-driven CDS-stacked section in Figure 2b, these conflicting dip situations are fully resolved: the interference of intersecting events is properly simulated, many new steep events show up. The S/N ratio is now slightly lower, but due to the more complete stack, this section is better suited as input for poststack migration (Soleimani et al., 2009). Finally, Figure 2c shows the first result obtained with the data-driven CDS approach. For this section, all contributions for all considered emergence angles are simply superimposed, without any weighting or thresholding based on coherence. Reflection events only receive energy from a small range of emergence angles. Thus, the strong continuous reflection events in the CRS stack result appear much weaker here. Instead, the section is dominated by a multitude of diffraction events because they receive energy from all emergence angles.

Conclusions. We have implemented and applied a model-based approach to the CDS stack method. The approach fully resolves the conflicting dip problem occurring in complex data and strongly emphasizes diffraction events. Thus, the model-based CDS stack section complements the usual stack section after a subsequent poststack depth migration as it helps to delineate discontinuities in the subsurface. This is relevant for situations in which the generation of velocity models sufficiently accurate for prestack depth migration is difficult or even impossible.

References

Mann, J. [2001] Common-Reflection-Surface stack and conflicting dips. In Extended abstracts, 63rd Conf. Eur. Assn. Geosci. Eng. Session P077.

Mann, J., Duveneck, E., Hertweck, T., and Jäger, C. [2003] A seismic reflection imaging workflow based on the Common-Reflection-Surface stack. J. Seis. Expl. 12(3), 283–295.

Mann, J., Jäger, R., Müller, T., Höcht, G., and Hubral, P. [1999] Common-Reflection-Surface stack – a real data example. J. Appl. Geophys. 42(3,4), 301–318.

Soleimani, M., Mann, J., Adibi Sedeh, E., and Piruz, I. [2010] Improving the seismic image quality in semi-complex structures in North East Iran by the CDS stack method. In Extended abstracts, 72nd Conf. Eur. Assn. Geosci. Eng. Session P398.

Soleimani, M., Piruz, I., Mann, J., and Hubral, P. [2009] Common-Reflection-Surface stack: accounting for conflicting dip situations by considering all possible dips. J. Seis. Expl. 18(3), 271–288.
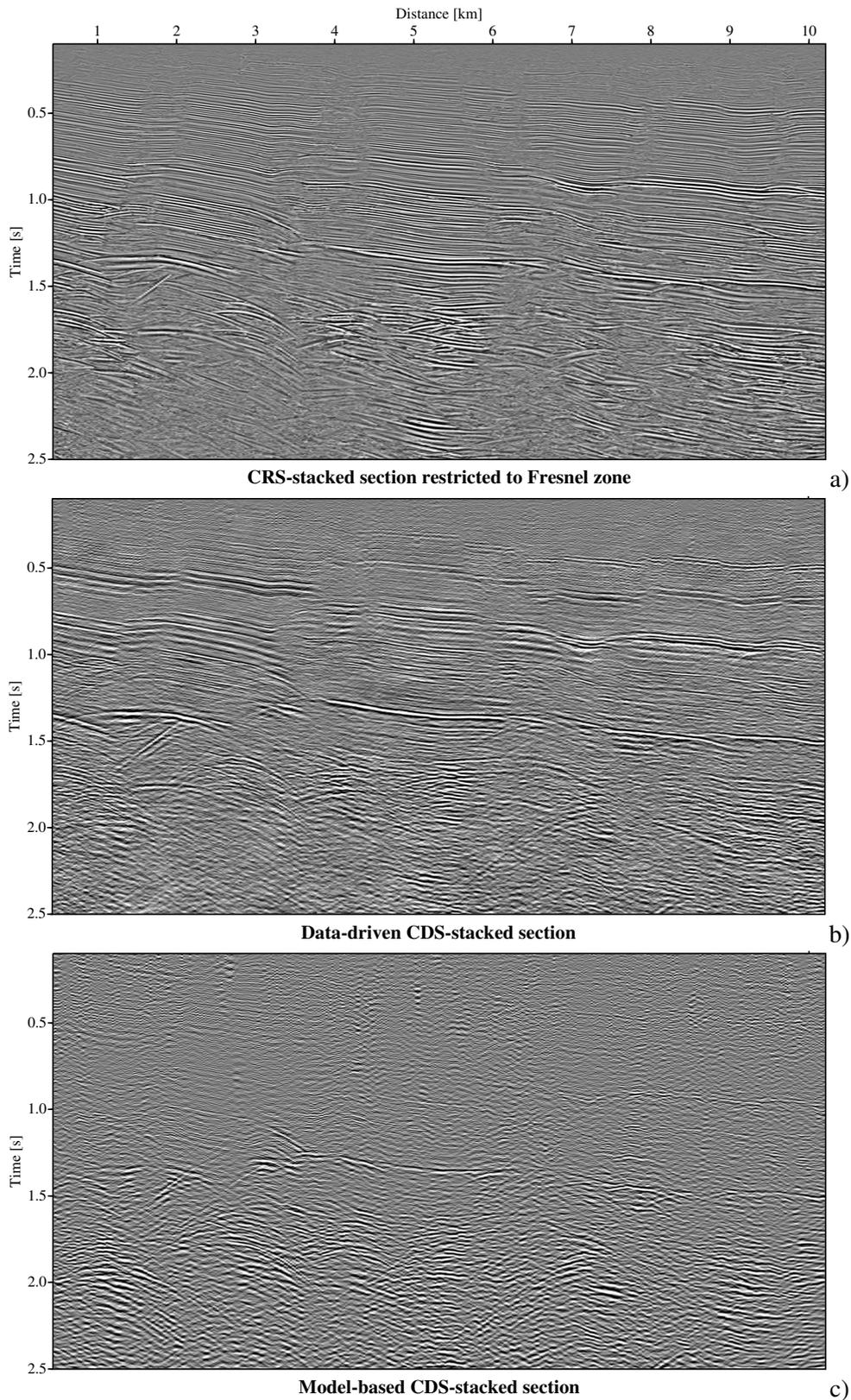
Figure 2: a) CRS-stacked section restricted to the projected first Fresnel zone. Note the artificial appearance with various truncated events. b) data-driven CDS-stacked section (modified after Soleimani et al., 2009). The interference of intersecting events has been simulated everywhere. c) model-based counterpart generated in an significantly smaller computation time. The process strongly pronounces diffraction events only partly seen in the other sections.